Available online at www.sciencedirect.com
SCIENCE DIRECT®
International Journal of Heat and Mass Transfer 48 (2005) 161–170
International Journal of HEAT and MASS TRANSFER
www.elsevier.com/locate/ijhmt

Jet impingement on a dimpled surface with different crossflow schemes

Koonlaya Kanokjaruvijit, Ricardo F. Martinez-botas *

Department of Mechanical Engineering, Imperial College London, Exhibition Road, South Kensington, London SW7 2AZ, United Kingdom

Received 1 March 2004
Available online 13 October 2004

Abstract

An eight-by-eight jet array impinging onto a staggered array of dimples at Reynolds number 11,500 was investigated by the transient wide band liquid crystal method. The distance between the perforated plate and the target plate was adjusted to be 2, 4 and 8 jet diameters to examine its effect on the heat transfer performance. Two dimple geometries of hemispherical and cusped elliptical were examined. Moreover, the effect of crossflow scheme on heat transfer was investigated: one-way, two-way and four-way spent air exits. All heat transfer results were normalized by those from a flat surface at the same condition.

Keywords: Dimple; Impingement; Crossflow; Jet-to-plate spacing; Dimple geometry

1. Introduction

Jet impingement is a mature technique, which has been examined by many researchers as a method of heat transfer enhancement in a variety of applications. There have been a number of attempts to complement jet impingement with other enhancing techniques such as crossflow, ribs and turbulators. Attempts have been made to optimize each method in order to obtain effective heat transfer with low pressure loss. In order to augment the heat transfer, the boundary layer has to be thinned or be partially broken and restarted. Protruding ribs have been used widely to enhance the heat transfer. However, the higher pressure loss, high maintenance and weight are the problems the application of ribs has. Dimpled surface has become into the consideration due to its potential in heat transfer augmentation, light weight, low pressure penalty and low maintenance.

Obot and Trabold [1] investigated the effect of spent air exit scheme or crossflow scheme on the heat transfer of impinging jets on a flat surface by unrestricting/restricting the spent air: minimum, intermediate and maximum crossflow schemes (or two-way and one-way exits, respectively). These were done in order to vary the degree of degradation due to the strength of the crossflow. As a result, they found that the minimum crossflow scheme showed the best performance followed by intermediate and maximum crossflows.

The concept of using dimples derives from that of the flow past a cylinder with shedding fashion. Beginning

* Corresponding author. Tel.: +44 20 7584 7241; fax: +44 20 7823 8845.
E-mail address: r.botas@imperial.ac.uk (R.F. Martinez-botas).

0017-9310/$ - see front matter © 2004 Elsevier Ltd. All rights reserved.
doi:10.1016/j.ijheatmasstransfer.2004.08.005

Nomenclature

c	thermal capacity of acrylic
D	jet diameter
h	heat transfer coefficient
H	distance measured from nozzle plate to flat portion of target plate
k	thermal conductivity of acrylic
Nu	Nusselt number, hD/k_{air}
T	temperature
X	spanwise distance of target plate
Y	streamwise distance of target plate

Greek symbol

ρ	density of acrylic plate

Subscripts

dimple	of dimpled surface
flat	of flat surface
i	initial
m	bulk
s	surface

with imprinted dimples on a golf ball investigated by Bearman and Harvey [2], two dimple geometries: hemispherical and hexagonal were tested on lift and drag. The hexagonal dimples were found induced higher lift but lower drag than the hemispherical ones, because there were discrete vortices shed into the boundary layer. Applying a dimpled surface to the parallel flow has been investigated by some researchers. Kerarev and Kozlov [3] studied the flow past a single hemispherical dimple of 150 mm diameter, and explained the flow pattern in terms of "sources" and "sinks". The heat transfer was enhanced by 1.5 times compared to a plane circle of the same imprinted diameter. The effect of density of a staggered-dimpled plate was examined by Afanasyev et al. [4]. They concluded that the density did not have an important effect on the flow hydrodynamic, but on the separation of temperature profile. The greater the density of the dimples on the streamline surface, the greater the deviation of the temperature profile was from the logarithmic law of wall. However, the heat transfer was increased by 30–40% without any significant increase in friction factor. They suggested that the viscous sublayer thickness was slightly decreased due to the concavities of the dimple. A heat transfer study of the flow past a staggered dimple passage was conducted by Moon et al. [5] using the narrow-band transient liquid crystal method. They stated that the dimpled passage enhanced heat transfer by 2.1 times that of a smooth passage, while the friction factor was only 1.6–2 times more. Chyu et al. [6] investigated the effect of dimple geometry by comparing the heat transfer results of hemispherical and tear-drop shaped dimples. The teardrop shaped dimples lead to higher heat transfer rates than the hemispherical dimples, but of course, induced a larger pressure loss due to their sharp angled part. The fluid mechanics of the flow past a staggered array of hemispherical dimples was examined by Mahmood et al. [7] using smoke-wire technique to visualize the flow. Vortex shedding was observed, and it leads to an enhancement of heat transfer of 1.85–2.89 times relative to a flat plate.

Dimple impingement has not yet been well-apprehended, especially the jet impingement on an array of dimples due to numerous complications. A single impinging jet onto a concave surface was visualized by Cornaro et al. [8] varying jet-to-plate spacing, which strongly influenced the flow dynamics. They found that at the larger spacing and low Reynolds number, stable coherent vortices existed, and the jet oscillated randomly about the stagnation point. However, at the closer spacing, vortex structures also occurred, and the flow along the surface oscillates in the axial direction. Nevertheless, the closer spacing also caused the recirculation after impinging and disturbed the oncoming flow. Gau and Chung [9] examined slot jet impingement on semi-cylindrical concave and convex surfaces varying the slot width to surface diameter ratios from 8 to 45 at Reynolds number from 6000 to 35,000. Both cases enhanced heat transfer beyond impingement on a flat plate. Ekkad and Kontrovitze [10] used a transient narrow band liquid crystal technique to investigate jet impingement onto a hemispherical dimpled surface with dimple diameter-to-depth ratios of 0.125 and 0.25. Their dimple size was designed for the jet to impinge completely within the dimple. Their results showed that the appearance of dimples did not complement the jet impingement, but reduced the heat transfer, unlike the application of dimples to the passage flow.

The goal of the current research was to study the heat transfer performance of jet impingement onto a dimpled surface. Reynolds number based on a single jet diameter was specified at 11,500. A ratio of jet diameter-to-dimple diameter of 0.59 was used. The measurement technique was the transient wide band liquid crystal method. Dimples were used as turbulence promoters. The effect of dimple geometry on heat transfer was investigated using conventional hemispherical dimples as well as a new geometry in the form of a cusped elliptical shape. All results were compared with those of a flat surface in order to explain the consequence of the usage of dimples. Furthermore, the effect of crossflow scheme was studied to

illustrate how each scheme affected the thermal transport.

2. Experimental apparatus and procedures

A schematic of the experimental apparatus is shown in Fig. 1. The air was supplied by a fan, and heated up by a 9-kW heater. A honeycomb sandwiched by two mesh screens installed inside the plenum chamber of the size 0.5×0.5 m was used in order to straighten the flow, so that the flow was more uniform than that before the honeycomb. The local flow rates were monitored across the plenum chamber in both directions before and after installing the honeycomb. The nozzle plate was located approximately 300 mm underneath the honeycomb, and the mesh size was less than 5×5 mm, the flow was uniform as might be expected. Due to the fact that the transient experiments were carried out, the heated flow inside the plenum chamber needed to settle before impinging onto the target plate, a drawer was introduced to divert the flow. When the flow rate and temperature of the flow inside the plenum chamber were stable, the drawer was pulled opened, and the bypass was closed allowing the flow to travel through the nozzle plate and impinge onto the target plate.

A target plate and its sidewalls were hung from the nozzle plate. The distance between the perforated plate and the target plate (H/D) was adjusted to be 2, 4 and 8 jet-diameters. Sidewalls made of acrylic plates were installed or removed when changing the crossflow schemes such as maximum, intermediate and minimum spent exits as shown in Fig. 2. After the jets impinge on the target plate, they accumulate, and form "crossflow" or "spent air", which leaves the plate towards the exit(s) depending on the exit scheme. The crossflow velocity profile is not shown here due to the fact that the mass flow rate from the plenum chamber is sufficient to calculate Reynolds number of a jet. For the minimum crossflow scheme, there was no sidewall, so the crossflow freely exited. Two sidewalls constrained the crossflow to leave in two opposite directions in the intermediate crossflow scheme. And the strong crossflow constrained by three sidewalls was forced to leave in one direction, and this formed the maximum crossflow scheme. A 10-mm thick nozzle plate of an eight-by-eight array of cylindrical holes with straight edges of diameter 10 mm was attached to the bottom plate of the plenum chamber. The alignments of the jet holes to dimpled plates are illustrated in Fig. 3.

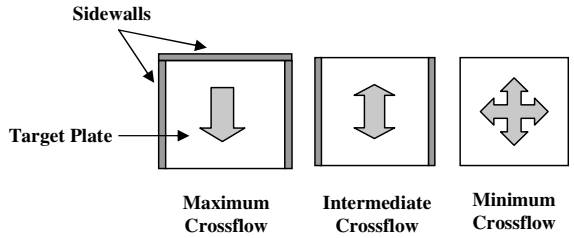

Fig. 2. Crossflow schemes formed by installing or removing sidewalls. Note that the arrows represent the crossflow directions.

Two dimpled plates with the same wetted area for each dimple were tested: hemispherical and cusped elliptical

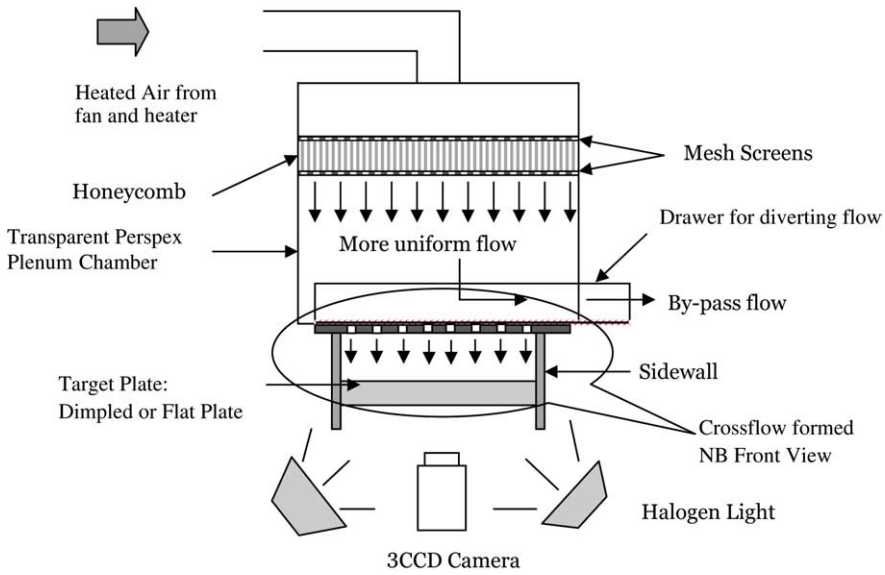

Fig. 1. Schematic of experimental appratus.

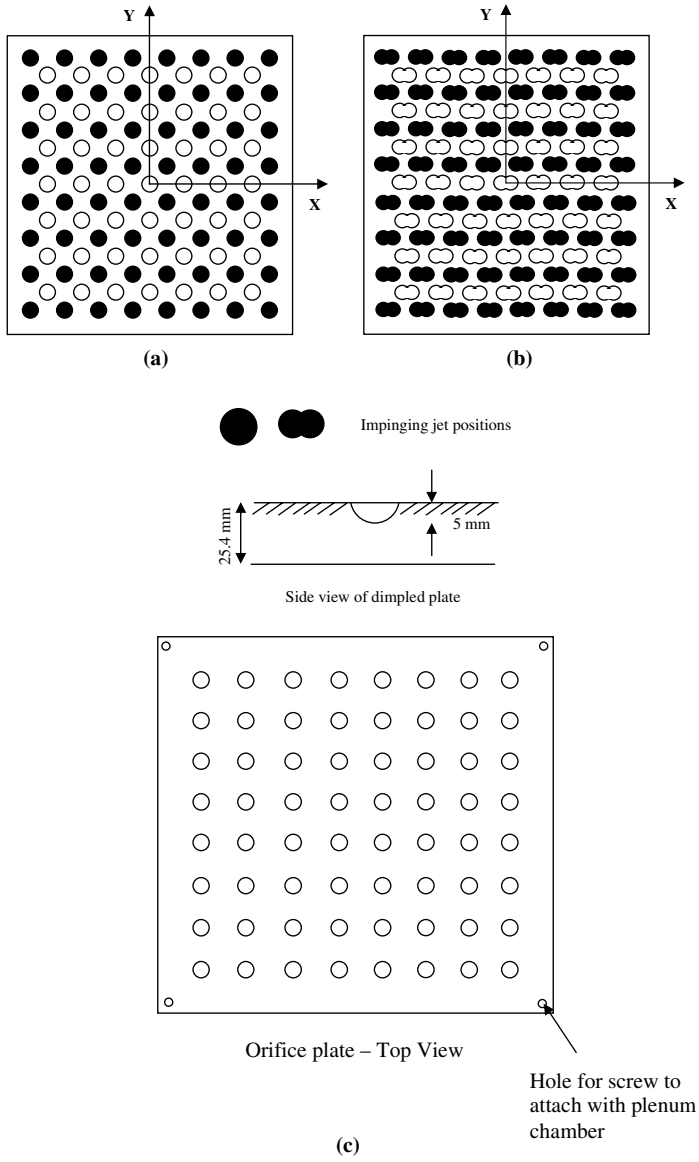

Fig. 3. Dimpled plates in both hemispherical and cusped elliptical dimpled shapes showing also the positions of impinging jets (not to scale). Black filled dimples represent the alignment to the jet holes. (a) Hemispherical shape; (b) Cusped elliptical shape and (c) Nozzle plate of straight holes and diameter 10 mm.

shapes. Both were manufacture in staggered pattern on a square Acrylic plate of the size $320 \times 320 \times 25.4$ mm, illustrated in Fig. 3. The diameter of a hemispherical dimple was 17 mm, and each circle diameter of a cusp was 14.5 mm with the center-to-center distance of 8.74 mm. The pitch of the dimples was 40 mm. Both plates were fabricated by using a ball mill and with the depth of 5 mm. A flat plate with the same dimension was also tested at the same conditions as a baseline. The cusped elliptical dimples were selected with the concept of the overlapping of two hemispherical dimples produced two sharp apices, which had potential of detaching the boundary layer better than round edges of regular hemispherical dimples as well as the consideration of simplicity in manufacturing. Note that the thickness of the target plates was designed economically under the assumption of one-dimensional conduction and from the correlation, $z = 2\sqrt{\alpha t}$ [11].

Liquid crystals with a temperature range of 35–45 °C, were applied on the acrylic target plate followed by black paint. A 3CCD camera was set up to take a picture from underneath with an off-axis fixed lighting

installation. In the current study, two 20-W halogen lights were employed. The liquid crystal calibration was carried out only on the flat portions of the dimpled plates due to the fact that the dimple areas were not taken into account due to the unavoidable accumulation of the liquid slurry at the bottom of the dimples when spraying. According to Camci et al. [12] and Wang et al. [13], hue is robust to the local light intensity and the illumination angle. It is also simple and monotonic function to the liquid crystal temperature, and, therefore, widely employed as a color index. The liquid crystal calibration of hue value against temperature was carried out for each target plate with the uncertainty within ±3%. The curve fitting and regression analysis provided the fifth order polynomial temperature–hue relationship in accordance with Yuen and Martinez-Botas [14] and [15].

Each camera image was transferred to a personal computer using a firewire lead, which transferred data directly from the camera to the computer without the usage of a frame grabber. Each experiment was filmed with the non-compression mode in order to receive the data as complete as possible. Only the natural compression from the camera was allowed.

Since the transient method was applied throughout the research, the well known solution to the 1D unsteady heat conduction equation was used:

$$\theta = 1 - \exp\beta^2 \operatorname{erfc}\beta \tag{1}$$

where

$$\theta = \frac{T_s - T_i}{T_m - T_i} \quad \text{and} \quad \beta = \frac{h\sqrt{t}}{\sqrt{\rho c k}}$$

Only the flat areas outside dimples were considered for the image post-processing. The areas inside the dimples were not taken into account, these areas were, therefore, ineffective or out of interest.

The experimental uncertainty throughout this study was within ±12.17% based on 95% confidence level. The highest uncertainty that might happen was the sum of uncertainties of temperature measured by liquid crystals, the initial and the bulk flow temperatures measured by thermocouples, the time measured for taking a single frame (which was 1/25 second regarding the PAL system from the camera) and the thermal products from the acrylic substrate, $\sqrt{\rho c k}$. As aforementioned, the temperature measured by liquid crystals has the uncertainty within ±3%. Thermocouples used in this study had the uncertainty of ±0.5 °C, which made the uncertainties of initial and bulk flow temperatures become ±2.5 and ±1%, respectively. The highest uncertainty of time was ±0.67%. Finally, the uncertainty of the thermal properties of the acrylic substrate was typically ±5%.

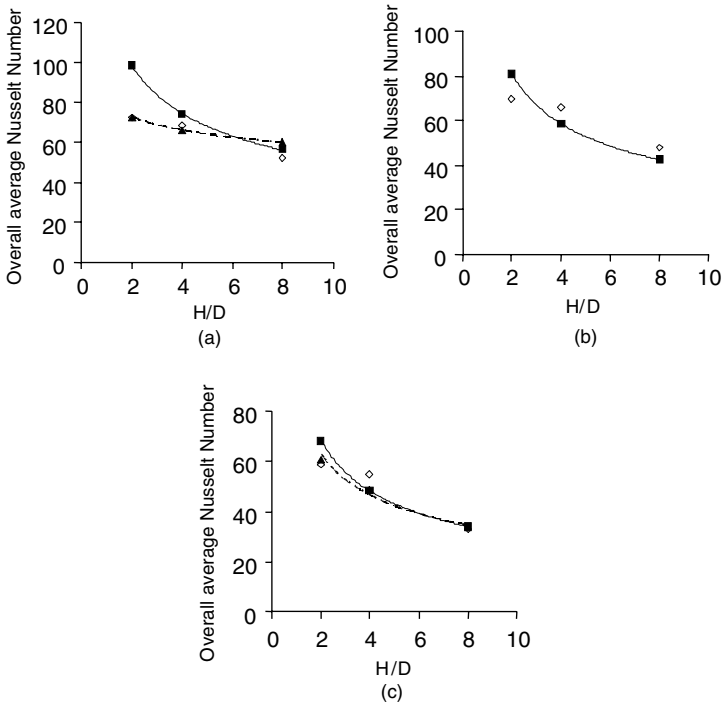

Fig. 4. Comparison to literature: (a) minimum crossflow scheme; (b) intermediate crossflow scheme and (c) maximum crossflow scheme. ◇ Present study, ■ Obot and Trabold [1]. (a) ▲ Andrews and Hussain [16]; (c) ▲ Huber and Viskanta [17].

3. Results and discussion

3.1. Overall average heat transfer of flat plate

The heat transfer results are presented as dimensionless Nusselt numbers at the specific Reynolds number of 11,500. Fig. 4 shows the comparison of the results of a flat plate from this research to the literature; they agree well. As expected, the minimum crossflow scheme led to the highest heat transfer enhancement, followed by the intermediate crossflow scheme, and the maximum crossflow scheme gave the lowest results. It has been clearly explained by other researchers that strong crossflow causes heat transfer degradation, especially near the exit area, where the crossflow affected the most. The heat transfer results from the flat plate will be used as a baseline for those from dimpled surfaces hereafter.

Fig. 5 shows the spanwise and streamwise average Nusselt numbers of the flat plate for H/D of 8 for all schemes. The sidewalls, which confided the spent air to exit for the intermediate and maximum schemes, led to the heat transfer reduction. The symmetry of the heat transfer patterns in both spanwise and streamwise directions occurred in the minimum and intermediate schemes as the sidewalls conducted the spent air to. However, in the maximum crossflow scheme, the stagnation peaks were shifted and reduced in the streamwise direction by the strong crossflow degradation.

3.2. Effect of crossflow scheme on dimpled surfaces

Throughout in this study, the jets impinged on dimples with the idea of employing the edges of dimples to thin the boundary layer, and enhance the heat transfer

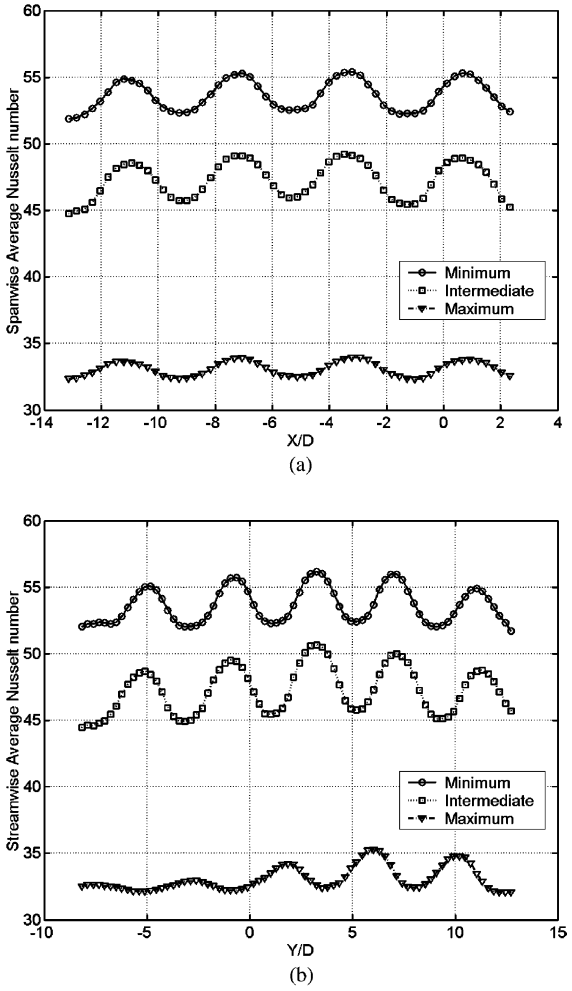

Fig. 5. Local average Nusselt numbers for flat plate at H/D of 8: (a) spanwise and (b) streamwise.

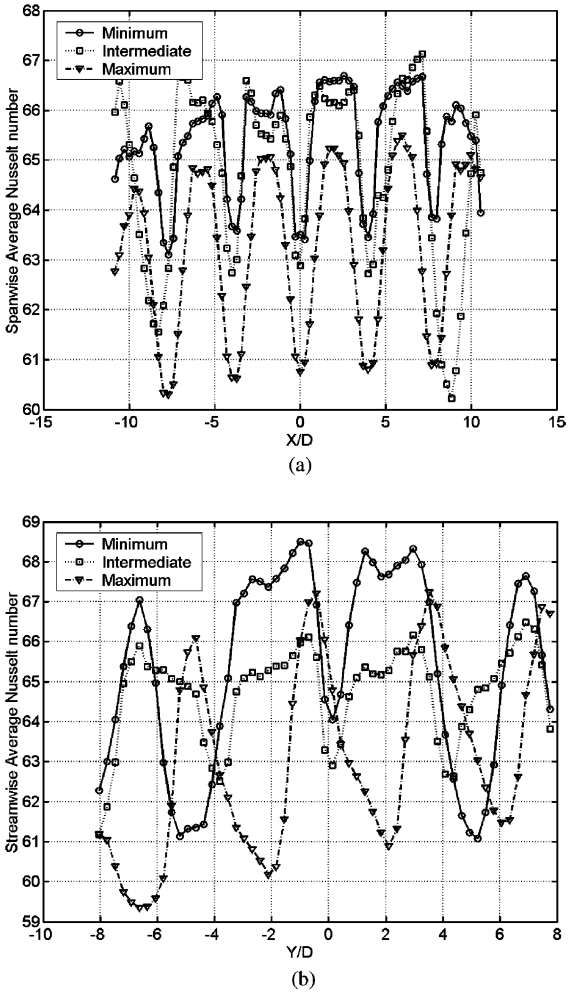

Fig. 6. Local average Nusselt numbers for hemispherical dimpled plate at $H/D = 2$: (a) spanwise and (b) streamwise.

of the flat portions between dimples. The lowest heat transfer was expected inside each dimple similar to the parallel flow past dimples investigated by Mahmood et al. [7] and to the study of Kesarev and Kozlov [3] on a single dimple.

At H/D of 2 in both dimple geometries, both the intermediate and maximum crossflow schemes conducted heat transfer slightly less than the minimum crossflow scheme as shown in Figs. 6 and 7. However, the improvement in heat transfer in the presence of crossflow occurred when compared with the flat surface case. The coupled effects of impingement and channel flow could explain this. The flow visualization on a planar jet impinging on a concave surface by Cornaro et al. [8] showed the vortices in radial and/or axial directions. For the minimum crossflow scheme, impingement dominated, since there was no sidewall to constrain the flow, but it freely exits. However, a recirculation region occurs inside the dimples, and small vortices are generated before subsequent breakdown [8]. After the jets impinged on the dimples, the crossflow was not strong enough to entrain the recirculating flow, while the spent air could not exit fast enough.

Fig. 8 shows the contour distribution of the Nusselt number on hemispherical dimples for the maximum crossflow with H/D of 8. Note that the flow direction is from the bottom upwards. As aforementioned, the areas inside dimples were not taken into account. In this case, the crossflow deflected the oncoming jets, and impacted on downstream halves of dimples. The channel flow was formed and overwhelmed the impingement. As a consequence the boundary layer was thinned downstream of dimples leading to heat transfer enhancement. The flat areas adjacent to the dimples show the highest heat transfer enhancement.

3.3. Effect of jet-to-plate spacing

The jet-to-plate spacing strongly affected the heat transfer results. For all crossflow schemes on the flat plate, the narrower the jet-to-plate spacing, the higher the heat transfer, which prior researchers have showed. For the dimpled plates, the heat transfer information did not follow the tendency of the flat plate, especially, for the minimum crossflow scheme in both dimpled plates. The highest Nusselt numbers occurred in the jet-to-plate spacing of 4 as shown in Fig. 9. The distance from the nozzle plate to the bottom of a dimple was 45 mm, which might be the end of the potential core. According to the flow visualization shown by [8], at the end of the potential core, the strong radial oscillation of the stagnation point accelerated the breakdown of the

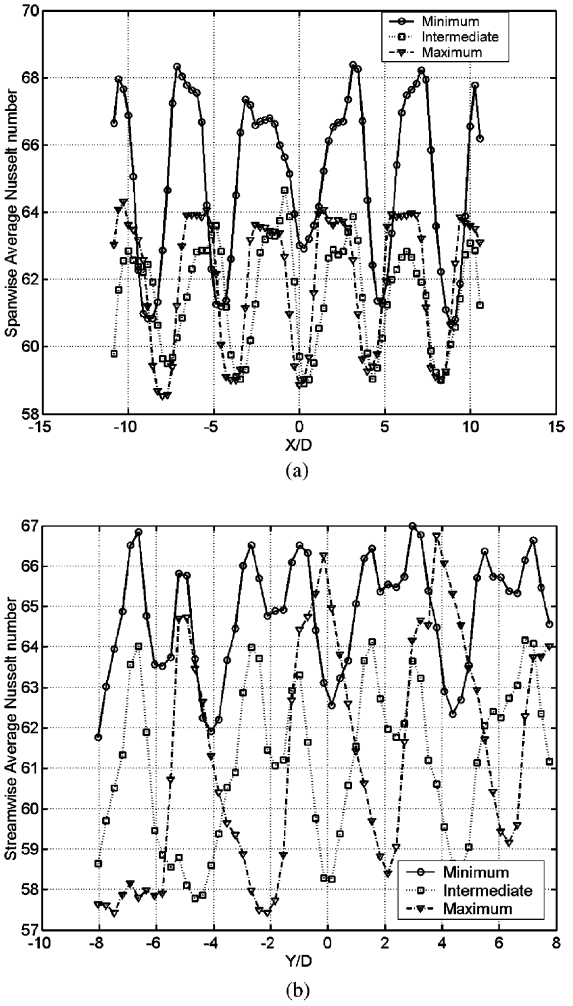

Fig. 7. Local average Nusselt numbers for cusped elliptical dimpled plate at $H/D = 2$: (a) spanwise and (b) streamwise.

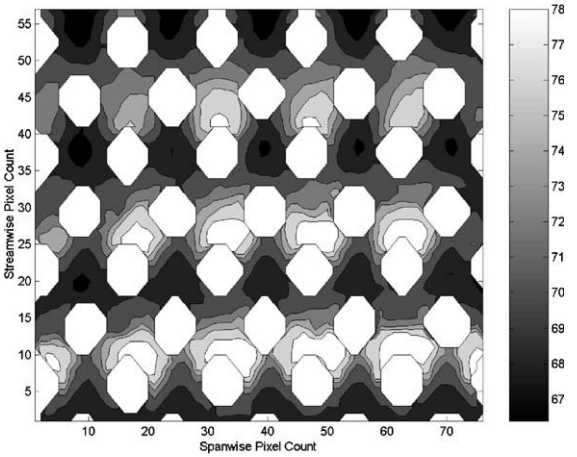

Fig. 8. Local Nusselt number distribution, hemispherical dimpled plate, maximum crossflow, $H/D = 8$. Note that the dimple areas are not taken into account.

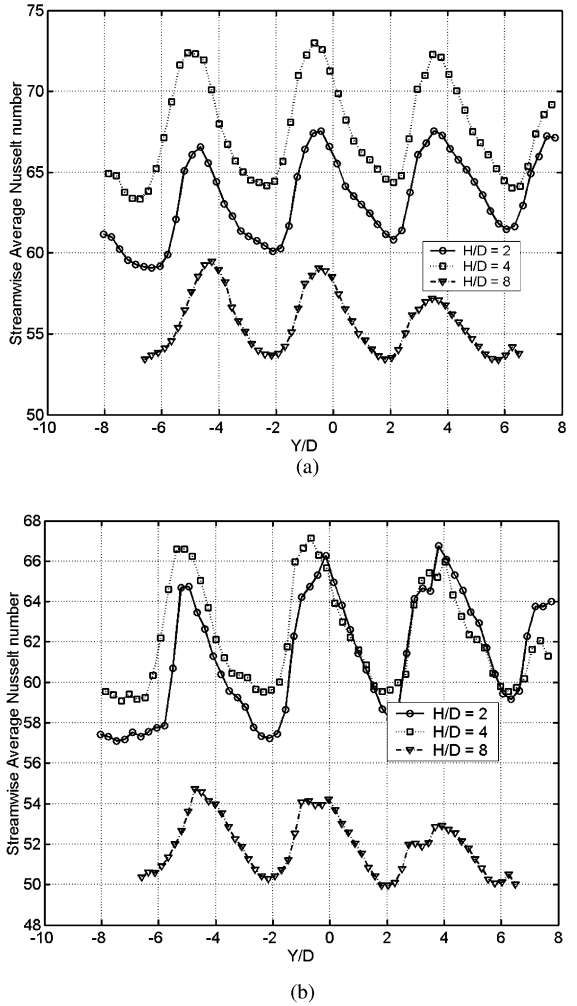

Fig. 9. Streamwise average Nusselt numbers for maximum crossflow scheme: (a) hemispherical dimples and (b) cusped elliptical dimples.

vortices that struck the surface, and this ruined the symmetry of the jet making it dissimilar to impingement on a flat plate. However, at the closer spacing, such as H/D of 2, even though the higher impact than other jet-to-plate spacing was expected, the strong recirculation might occur inside the dimples, and without the powerful channel flow formed for the freely exit scheme, the recirculating flow could not escape fast enough from each dimple. Therefore, the heat transfer measured from the flat portions of this case presented lower than H/D of 4, which is clearly seen for the hemispherical dimples.

3.4. Effect of dimple geometry

Both dimple geometries were designed based on the same wetted cross-sectional area or equivalent diameter with the same depth. Fig. 10 shows the comparison of

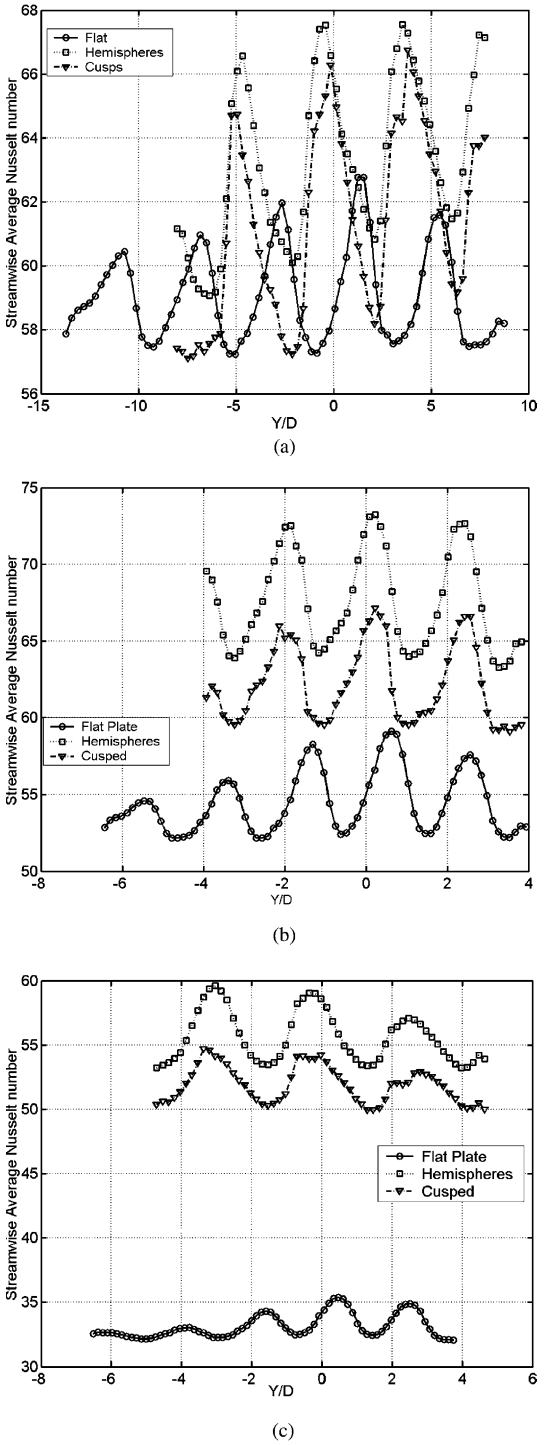

Fig. 10. Plots of streamwise average Nusselt numbers of both dimple geometries compared to those of flat plate for maximum crossflow scheme: (a) $H/d = 2$; (b) $H/d = 4$ and (c) $H/d = 8$.

the streamwise average Nusselt numbers for the maximum crossflow scheme at all jet-to-plate spacing of all

geometries. Note that the crossflow direction is from the right to left. The strong crossflow in the maximum crossflow scheme deflected the peaks of dimpled surfaces differently from the flat surface because from the video images showed that the channel effect shifted the oncoming jets to impact on the downstream halves of the dimples, and the higher heat transfer occurred at the higher crossflow amount. This caused the heat transfer maximal peaks to manifest on the downstream and minimal peaks on the upstream dimple halves.

For H/D of 2, the hemispherical dimples performed slightly better than the cusped elliptical dimples by 2.79% on average, 10.78% for H/D of 4 and 6.70% for H/D of 8. This might be because when the jets impinged on the hemispherical dimples, the recirculation inside both dimples that formed a cusped elliptical dimple was less severe than that inside each cusped elliptical dimple. In addition, the potential core was possibly slightly longer than four jet diameters as mentioned in the previous section. Each jet impinged on an intersection between two dimples that formed a cusped ellipse, and this could split the flow into two parts, which later produced a recirculating flow in each dimple. The two rolling-up recirculations disturbed the oncoming jet. However, since the three sidewalls constrained the spent air to form a channel flow, this might hasten the recirculation flow to shed along the crossflow. Hence, the degradation was not as severe in this shape compared to the other crossflow schemes. H/D of 8 for both geometries performed better than the other two spacings. The circulation inside each dimple, of course, was less strong and the edges of dimples might help thinning the boundary layer more effectively. Further flow visualization is needed to complete this physical explanation.

Nevertheless, in terms of economy, manufacturing and performance, the hemispherical shape is more attractive than the cusped elliptical shape. There are more parameters to determine the optimum such as dimple depth, ratio of jet diameter to dimple diameter (curvature) and position of impinging jets on the dimpled plate.

3.5. Overall average Nusselt numbers of dimples plates

Throughout the study, the jets impinged on dimples, and the areas inside were not taken into account as mentioned in the previous section. However, the video exhibited that the lowest heat transfer occurred inside each dimple. In the minimum and intermediate crossflow schemes for H/D of 2, the presence of dimples did not help, but reduced the heat transfer by 10%. With the jet-to-plate spacing of 4 for minimum crossflow, the overall average heat transfer of the impingement on dimples was not different from that of the flat plate. By overall average, the heat transfer was more enhanced with the maximum crossflow and larger jet-to-plate spacing. From the prior researches in augmenting heat

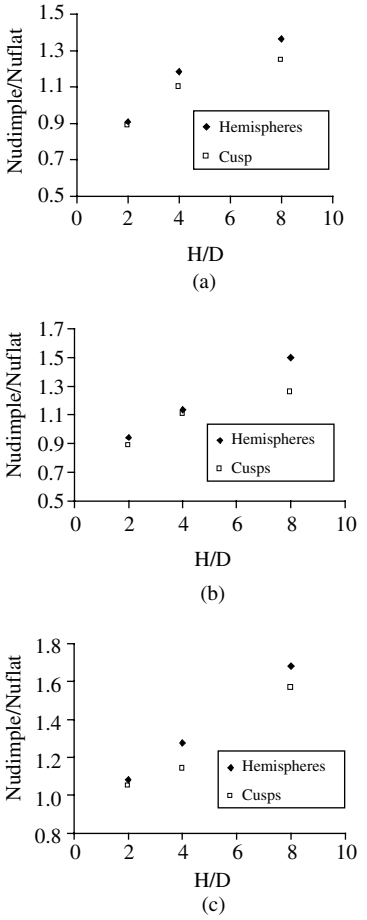

Fig. 11. Overall average normalized Nusselt numbers: (a) minimum crossflow; (b) intermediate crossflow and (c) maximum crossflow.

transfer of parallel flow using dimples, it could be inferred on the dimple impingement that the crossflow that formed a channel flow would have made a greater contribution of heat transfer enhancement. For the intermediate crossflow scheme, the dimpled plates enhanced heat transfer by 10% for H/D of 4, and 30–50% for H/D of 8 compared to that of the flat plate. The heat transfer was increased with the dimple application for the maximum crossflow schemes from 56% to 68%. The flow mechanism of dimple impingement might be considered as a coupled effect of jet impingement and channel flow with vortex shedding occurred in the staggered dimple array as mentioned in the prior sections. At the higher jet-to-plate spacings (4 and 8), compared to a flat plate, the heat transfer was more enhanced with the presence of dimples. The potential core occurred possibly at the end of H/D of 4, in addition, the depth of each dimple ensured the end of the potential core was reached. The dimples aided the impingement by

thinning or disturbing the boundary layer. However, the recirculation inside dimples was also concerned for degrading the heat transfer, especially the results shown in H/D of 2 (Fig. 11).

4. Conclusions

Impingement onto dimples performed best with the maximum crossflow scheme and larger jet-to-plate spacing due to the coupled effect of impingement and channel flow. The heat transfer on the downstream half of a dimple edge was higher than the upstream half. This occurred in maximum crossflow scheme, however, in minimum and crossflow schemes, the impingement overwhelmed the channel flow. For the intermediate crossflow scheme, either phenomenon could not perform at its high capacity, but seems to act moderately.

Since the jet impingement on dimples caused the recirculation inside the dimples, and this affected enormously on the case of narrow jet-to-plate spacing ($H/D = 2$), the heat transfer was aggravated comparing to that of the flat plate. However, the channel flow formed by the intermediate and maximum crossflow schemes helped diminishing this deterioration especially on H/D of 4 and 8.

Finally, the investigation on the effect of dimple geometry showed that hemispherical and a cusped elliptical dimple did not perform immensely differently. However, comparing in terms of economy, manufacturing and pressure loss, the hemispherical shape should be a better choice. Nevertheless, since the application of dimpled surface to jet impingement has just begun recently, the optimum of some parameters should be researched such as dimple depth, ratio of jet diameter to dimple diameter (curvature) and position of impinging jets on the dimpled plate as well as the qualitative flow visualization.

References

[1] N.T. Obot, T.A. Trabold, Impingement heat transfer within arrays of circular jets. Part 1: effects of minimum, intermediate, and complete crossflow for small and large spacings, J. Heat Transfer 109 (November) (1987) 872–879.
[2] P.W. Bearman, J.K. Harvey, Golf ball aerodynamics, Aeronaut. Quart. May (1976) 112–122.
[3] V.S. Kesarev, A.P. Kozlov, Convection heat transfer in turbulized flow past a hemispherical cavity, Heat Transfer Res. 25 (2) (1993) 156–160.
[4] V.N. Afanasyev, Ya.P. Chudnovsky, A.I. Leontiev, P.S. Roganov, Turbulent flow friction and heat transfer characteristics for spherical cavities on a flat plate, Exp. Thermal Fluid Sci. 7 (1993) 1–8.
[5] H.K. Moon, T. O'Connell, B. Glezer, Channel height effect on heat transfer and friction in a dimpled passage, ASME Paper, 99-GT-163.
[6] M.K. Chyu, Y. Yu, H. Ding, J.P.,Downs, F.O. Soechting, Concavity enhanced heat transfer in an internal cooling passage, ASME Paper, 97-GT-437.
[7] G.I. Mahmood, M.L. Hill, D.L. Nelson, P.M. Ligrani, Local heat transfer and flow structure on and above a dimpled surface in a channel, ASME International Gas Turbine and Aeroengine Congress and Exhibition, Germany, May 8–11, 2000.
[8] C. Cornaro, A.S. Fleischer, R.J. Goldstein, Flow visualization of a round jet impinging on cylindrical surfaces, Exp. Thermal Fluid Sci. 20 (1999) 66–78.
[9] C. Gau, C.M. Chung, Surface curvature effect on slot-air-jet impingement cooling flow and heat transfer process, J. Heat Transfer 113 (1991) 858–864.
[10] S.V. Ekkad, D. Kontrovitz, Jet impingement heat transfer on dimpled target surfaces, Int. J. Heat Fluid Flow 23 (1) (2002) 22–28.
[11] D.L. Schultz, T.V. Jones, Heat-transfer measurements in short-duration hypersonic facilities, AGARD-AG-165, 1973.
[12] C. Camci, K. Kim, S.A. Hippensteele, A new hue capturing technique for the quantitative interpretation of liquid crystal images used in convective heat transfer studies, J. Turbomach. 114 (1992) 765–775.
[13] Z. Wang, P. Ireland, T.V. Jones, A colour image processing system for transient liquid crystal heat transfer experiments, ASME Paper, 94-GT-290.
[14] C. Yuen, R.F. Martinez-Botas, Film cooling characteristics of a single holes at various streamwise angles. Part 1: effectiveness, Int. J. Heat Mass Transfer 46 (2003) 221–235.
[15] C. Yuen, R.F. Martinez-Botas, Film cooling characteristics of a single holes at various streamwise angles. Part 2: heat transfer coefficient, International Journal of Heat and Mass Transfer 46 (2003) 237–249.
[16] G.E. Andrews, C.I. Hussain, Impingement cooling of gas turbine component, Proceeding of Tokyo International Gas Turbine Congress and Exhibition, 1983.
[17] A.M. Huber, R. Viskanta, Effect of jet-jet spacing on convective heat transfer to confined, impinging arrays of axisymmetric air jets, Int. J. Heat Mass Transfer 37 (18) (1994) 2859–2869.